Title	A six-compound, high performance gasoline surrogate for internal combustion engines: Experimental and numerical study of autoignition using high-pressure shock tubes
Author(s)	Cancino, L.R.; da Silva Jr., A.; De Toni, A.R.; Fikri, M.; Oliveira, A.A.M.; Schulz, C.; Curran, Henry J.
Publication Date	2019-10-25
Publication Information	Cancino, L. R., da Silva, A., De Toni, A. R., Fikri, M., Oliveira, A. A. M., Schulz, C., & Curran, H. J. (2020). A six-compound, high performance gasoline surrogate for internal combustion engines: Experimental and numerical study of autoignition using high-pressure shock tubes. Fuel, 261, 116439. doi:https://doi.org/10.1016/j.fuel.2019.116439
Publisher	Elsevier
Link to publisher's version	https://doi.org/10.1016/j.fuel.2019.116439
Item record	http://hdl.handle.net/10379/16488
DOI	http://dx.doi.org/10.1016/j.fuel.2019.116439

A six-compound, high performance gasoline surrogate for internal combustion engines: Experimental and numerical study of autoignition using high-pressure shock tubes

L.R. Cancino[a,b,*], A. da Silva Jr[a,c], A.R. De Toni[b], M. Fikri[d], A.A.M. Oliveira[b], C. Schulz[d], H.J. Curran[e]

[a] *Internal Combustion Engines Laboratory, Automotive Engineering, Federal University of Santa Catarina - LABMCI/EMB/CTJ/UFSC, Joinville/SC, CEP 89219-600, Brazil*

[b] *Combustion and Thermal Systems Engineering Laboratory, Mechanical Engineering, Federal University of Santa Catarina - LABCET/EMC/CTC/UFSC, Florianopolis/SC, CEP 88040-900, Brazil*

[c] *Technische Hochschule Ingolstadt Mechanical Engineering Center of Applied Research ZAF, Esplanade 10, Ingolstadt D-85049, Germany*

[d] *Institute for Combustion and Gas Dynamics - Reactive Fluids, University of Duisburg-Essen - IVG/UDE, 47048 Duisburg, Germany*

[e] *Combustion Chemistry Centre, National University of Ireland Galway - C3/NUIG, University Road, Galway, H91 TK33, Republic of Ireland*

Abstract

This paper presents experimental and modeling data for the autoignition of a novel, six-component, high performance gasoline surrogate fuel comprising ethanol, *n*-heptane, *i*-octane, 1-hexene, methylcyclohexane, and toluene (AL-P-I-O-N-A). Experimental tests are conducted in two high-pressure shock tubes to determine the ignition delay time as a function of pressure, temperature and equivalence ratio. Ignition delay times were measured at 10 and 30 bar in the temperature range from 749 to 1204 K and equivalence ratios ranging from 0.35 to 1.30. A modified Arrhenius equation is defined to mathematically describe the ignition delay time of the proposed surrogate. For experimental data with temperatures higher than 900 K, a multiple linear regression identified the pressure dependence exponent of 0.72 and stoichiometry dependence exponent of 0.62, as well as a global activation energy of ≈109 kJ/mol. A simplistic approach to mechanism reduction based on the elimination of reactions with no relevant rate of progress was used in order to reduce an extensive detailed kinetics model (hierarchically constructed with more than 17800 reactions). The reduced detailed kinetics model with 4885 elementary reactions among 326 chemical species was used for numerical simulations. Comparisons between the experimental and numerical data are favorable, with the predictions using the reduced kinetics model differing by less than 0.056% when compared to the complete mechanism. It was observed that for low temperatures the proposed reduced kinetics model agrees only qualitatively with the measurements. In order to understand the likely cause of this discrepancy a brute force sensitivity analysis on IDT was performed, elucidating the more influencing reactions on the ignition delay times. The experimental data obtained in this research was compared to available data in the literature in terms of anti-knock index (AKI) and for a scaled pressure of 30 bar (τ_{30}) at a stoichiometric composition. A modified Arrhenius equation was then fitted and an AKI dependence exponent of -1.11 was obtained, inferring that the higher the AKI the higher the IDT, independent of fuel composition at temperatures lower than the NTC region. This trend should be confirmed by further studies.

Keywords: Multicomponent gasoline surrogate, High-pressure shock tube, Reduced chemical kinetics mechanism, Brute force sensitivity analysis.

Contents

*Corresponding author
Email address: leonel.cancino@labmci.ufsc.br (L.R. Cancino)

1. Introduction

Vehicle propulsion technologies employing internal combustion engines (ICE) are being pushed to a higher level of performance, mainly because of future emissions regulations. The European Commission (EC) has adopted a new regulatory proposal establishing that the average emissions of the EU fleet of new cars must drop by 15% in 2025 and by 30% in 2030, compared to their respective limits in 2021 [1]. In order to comply with these regulations and satisfy well-to-wheel sustainability requirements, the research in internal combustion engines has focused in a host of strategies in new combustion concepts, control and after-treatment systems [2]. The combustion solutions for light and medium vehicles include the use of alternative fuels, such as biofuels [3], compressed natural gas (CNG) [4], and liquid petroleum gas (LPG) [2], and advanced combustion strategies, such as homogeneous charge compression ignition (HCCI) [5, 6, 7, 8, 9, 10, 11], reactivity-controlled compression-ignition (RCCI) [12], and lean combustion, high-compression ratio, spark controlled, gasoline compression ignition (GCI) [13].

HCCI engines provide a higher thermal efficiency compared to spark ignition (SI) and compression ignition (CI) engines, producing lower levels of nitrogen oxides (NO_x) and particular matter (PM), as well as near-zero soot emissions [14, 15]. One of the major challenges in HCCI is to control the timing of the auto-ignition event, which is responsible for initiating the CI combustion process [14, 15, 16]. In SI engines auto-ignition may cause an abnormal combustion known as knocking, which affects the engine's overall performance [17]. A fuel with a higher knocking resistance allow the engine to run at higher efficiency at high loads when knocking is limiting [18, 19]. With such high performance gasoline fuels, the control of compression ratio, valve timing and variable intake system allow to take advantage of the higher fuel knocking resistance [20]. Therefore, the formulation of new high performance gasoline fuels requires to investigate the dependence of ignition delay time on temperature and pressure in order to predict the conditions that lead to the start of combustion in HCCI mode, or the onset of knocking in SI engines.

The ignition delay time (IDT) is defined as the time interval from the elapsed time when the air/fuel mixture reaches a pressure and temperature condition sufficient to ignite it to when the mixture actually auto-ignites [21, 22]. Mathematical correlations can be used to predict the IDT of a practical fuel. These equations are based on traditional Arrhenius expressions and may have from three to dozens of parameters [23, 24]. For different kinds of fuels, in addition to temperature and pressure, some researchers have proposed equations involving the use of other parameters such as oxygen percentage [24], octane number (ON) [25], equivalence ratio [26], carbon chain length [27], among others. In this study, the ignition delay time correlation is expressed according to a modified Arrhenius expression [28, 29] as

$$\tau_{\mathrm{ing}} = A \times \exp\left(\frac{E_a}{RT}\right) \times p^{-x} \times \phi^{-y}, \qquad (1)$$

where A is the pre-exponential factor, E_a is the global apparent activation energy, R is the universal gas constant, x and y are the pressure and stoichiometry dependence coefficients respectively. Eq. 1 is advantageous because its input values are parameters directly measured on the test facilities, and because it is known to provide a good curve-fit of IDT measurements especially at high temperatures ($T > 1000$ K) [21, 29].

A single Arrhenius correlation is not able to describe a two-stage ignition since it does not capture the cool flame phenomenon [30, 31], which is exhibited by paraffin class fuels and varies significantly with the hydrocarbon structure. Normal paraffins, such as n-heptane and n-decane, give strong cool flames, while branched chain paraffins are more resistant to ignition [30]. The cool flame phenomenon is usually associated with negative temperature coefficient (NTC) behavior, in which the reaction rate decreases with increasing temperature in the intermediate temperature region (650 K $< T <$ 1000 K) [32].

The ignition delay time of a fuel mixture can be determined in different types of test facilities, such as high-pressure shock tubes (HPST) and rapid compression machines (RCM) [33]. Studies of practical gasoline fuels are quite scarce [34] given that it is very difficult to investigate them in any great detail, as these fuels comprise approximately one hundred different chemical species, making any detailed combustion modeling / characterization process very difficult to achieve [35]. Chemical surrogates allow to approximate the thermal ignition of the real fuels. Many researchers have conducted IDT measurements for the development and validation of global and detailed chemical kinetics models for fuel surrogates with great success [35, 36] and this is the strategy adopted here.

Studies of practical gasoline fuels are quite scarce [34] given that it is very difficult to investigate them in any great detail, as these fuels comprise approximately one hundred different chemical species, making any detailed combustion modeling / characterization very difficult [35].

Additionally, there are few studies with high performance (AKI > 90) gasolines, with most data obtained from engine tests [37, 38, 39]. Agbro *et al.* [40] employed a rapid compression machine to obtain IDTs of a gasoline/*n*-butanol blend and a TRF (RON = 95) surrogate for $\phi = 1.0$ at 20 bar and 678−858 K. Results showed that the effect of *n*-butanol as an octane enhancer were above what should be expected based on a simple linear blending law. Sarathy *et al.* [41] performed extensive testing of two FACE (Fuels for Advanced Combustion Engines) gasolines, FACE F and FACE G, using both an RCM and a shock tube for $\phi = 0.5$ and 1.0, at 20 and 40 atm at temperatures from 650 to 1270 K. Results at temperatures above 900 K were similar for both fuels but intermediate temperature data showed stronger NTC behavior for the FACE F gasoline, which had a lower octane sensitivity. Simulations performed with various proposed surrogates demonstrated a significant kinetic coupling between cycloalkanes and aromatics, affecting the radical pool population.

In this work, a novel, six-compound gasoline surrogate with anti-knock index of 95.5 (AKI = (RON + MON)/2) is developed to emulate a high-performance gasoline. This surrogate has 27 % vol. ethanol in the composition, thus being representative of a potential Brazilian high performance gasoline with a relatively high oxygenated biofuel content [42]. The ignition delay time for this surrogate is measured in two different high-pressure shock tube facilities, a reduced chemical kinetics mechanism is developed and the important reactions are elucidated using sensitivity analysis. The results may be used for engine combustion development and also as a baseline for future fuel optimization.

1.1. Gasoline surrogates

Practical gasoline contains different kinds of substances distributed mainly among linear and branched straight-chain alkanes, cyclo-alkanes, aromatics, and olefins [43]. Gasoline surrogates are formulated to represent a practical gasoline while simultaneously maintaining its chemical and physical characteristics, such as ignition delay time, burning velocity, viscosity, density, vaporization, octane rating, and emissions [35, 44, 45], as well as spray behavior (spray break-up, penetration and dispersion angle) [46, 47].

In the formulation process of a surrogate, a reliable approach to ensure the prediction of numerous combustion targets of the real fuel is to include one or more components from each hydrocarbon class in the surrogate, ensuring that at least one molecular structure of each class is represented [44].

A single component gasoline surrogate such as *iso*-octane is able to reproduce flame propagation characteristics [48], however it would be inconsistent to choose this single compound to represent a practical fuel with a research octane number (RON) higher than 100. On the other hand, a five-component gasoline surrogate might be able to predict simultaneously a practical fuels RON value in addition to its ignition delay time [35, 49, 42]. Thus, in recent years there has been a growing interest in the formulation of ternary mixtures (*n*-heptane/*iso*-octane/toluene) and other multi-component mixtures, spanning the carbon number range from C_4 to C_{10} [50].

1.2. Chemical groups used for gasoline surrogates

A multi-component gasoline surrogate is usually formed by mixing four or more species comprising the most common hydrocarbon compounds in a practical fuel. In the literature the compounds frequently used are: linear paraffin (*n*-pentane or *n*-heptane), branched paraffin (*iso*-pentane or *iso*-octane), aromatic (toluene), naphthene (cyclopentane, cyclohexane or methylcyclohexane) and olefin (1-hexene, 1-pentene or *di-iso*-butylene) [36, 45, 49, 42, 51, 52, 53, 54]. Oxygenate surrogates additionally include an oxygenated compound (ethanol, butanol, MTBE, ETBE, etc.) [42, 50, 55].

Alcohols (AL), especially ethanol, are added to practical gasoline mainly to reduce both dependence on fossil fuels and pollutants emission [56]. Ethanol addition leads to a significant reduction in hydrocarbon (HC) and NO_x emissions [57]. Moreover, as ethanol has a high knock resistance, it can increase the overall octane rating of the ethanol-containing gasoline [42, 58].

In a practical gasoline the *n*-paraffinic (P) content is usually in the range from 7 to 14 mol.%, while *iso*-paraffins (I) are found in the range from 29 to 45 mol.% [45]. Paraffins, particularly *n*-paraffins, have a unique low-temperature chemistry that can lead to knock in SI engines and may facilitate ignition in HCCI engines [59]. The knocking tendency of *n*-paraffins increases with the length of the carbon chain, while *iso*-paraffins present a decreased knock tendency because of the side chains, especially when the methyl groups ($\dot{C}H_3$) are found in the second from the end or center position of the basic carbon chain [30].

Olefins (O) are hydrocarbon compounds with one or more carbon double bonds and are normally present in gasoline in small quantities, around 3 to 7 mol.% [45]. One double bond has little antiknock effect, while the presence of two or three bonds considerably increases the antiknock effect [30]. Because of their chemical structure, olefins can increase the reactivity of a gasoline as well as improve the gasoline octane number [60, 61]. Naphthenes (N) are saturated hydrocarbons that contain one or more rings, each of which may have one or more paraffin side chains [62].

Aromatics (A) are similar to naphthenes, but they contain a resonantly-stabilized unsaturated ring core [63]. Naphthenes are present in gasoline generally in the range from 1 to 20 mol.%, while aromatics are found in concentrations up to 35 mol.% [45]. Aromatics have a greater knock resistance than their corresponding sized naphthenes. In both groups of fuels the presence of two or more double bonds appreciably increases a fuels resistance to knock [30].

1.3. The GSBR1 (AL-P-I-O-N-A) gasoline surrogate

The present study proposes a novel, six-compound gasoline surrogate (dubbed GSBR1) to emulate a high performance gasoline. This surrogate has a measured anti-knock index of 95.5 [RON = 101.5, MON = 89.5] (Bontorin, A.C.B; Rouge, A; Oliveira, E.J. CENPES / PETROBRAS - Personal communication, 2019). Additionally the GSBR1 has 27 vol.%. ethanol in the composition, modeling a potential Brazilian high performance gasoline [42]. Table 1 shows the compounds as well as the volumetric percentage on mixture. All compounds were acquired from Sigma-Aldrich®.

Table 1: Composition of the gasoline surrogate GSBR1 proposed in this work

Group	Species	CAS Number	Purity (%)	Concentration (vol.%)
AL	Ethanol	64-17-5	≥99.5	27.0
P	*n*-Heptane	142-82-5	≥99.0	11.5
I	*i*-Octane	540-84-1	≥99.0	30.0
O	1-Hexene	592-41-6	≥99.0	5.0
N	MCH	108-87-2	≥99.0	7.0
A	Toluene	108-88-3	≥99.9	19.5

MCH: Methylcyclohexane
AL: Alcohols, P: *n*-Paraffins, I: *i*-Paraffins, O: Olefins
N: Naphthenes, A: Aromatics

2. Experimental approach

Two experimental facilities were used in this work, which are briefly described in the following.

2.1. High-pressure shock tube at IVG/UDE

The experimental facilities and procedures are described in earlier studies [52, 64, 65, 66, 67]. Gas mixtures were prepared by injecting the liquid gasoline surrogate mixture into an evacuated, heated stainless-steel mixing vessel, with subsequent complete evaporation. The total amount of fuel mixture and the added air were controlled manometrically in order to ensure the desired equivalence ratio. The mixture was stirred for two hours. All of the experiments were performed with the shock tube, the mixing vessel and all connecting gas lines pre-heated to 50°C. The shock speed was measured over two intervals using three piezo-electric pressure gauges. Pressure data were recorded with a time resolution of 0.1 μs.

All ignition delay times shown in this work were determined by extrapolating the steepest increase of the CH* chemiluminescence emission (at 431 nm) signal to its zero level on the time axis as shown in Figure 1(a). To account for the appearance of a cool flame, a second photomultiplier (PMT) was operated to measure CH_2O chemiluminescence in the 400 to 450 nm wavelength range. The estimated uncertainty in reflected shock temperature is less than ±25 K. The experiments were carried out using synthetic air containing 79% N_2 and 21% O_2. The driver gas was mixed in-situ by using two high-pressure mass-flow controllers. Helium was used as the main component and argon was added to match the acoustic impedance of the test gas. Concentrations of 5 to 20% Ar in He were required to generate tailored shock waves.

2.2. High-pressure shock tube at C3/NUIG

The high-pressure shock tube at C3/NUI Galway has been described in detail previously [34, 68, 69, 70] and is only briefly discussed here. This facility consists of a stainless steel tube of 8.76 m in length, with an internal diameter of 6.3 cm. A double-diaphragm section divides the shock tube into a 3 m long driver section and 5.73 m driven section. Aluminum plates were used as diaphragms in all experiments, with thicknesses varying from 1.0-1.4 mm depending on the desired temperature behind the shock wave T_5. The driver gas used was helium, with the eventual addition of nitrogen to achieve tailored driver gas conditions which allow for longer test times [71].

The diagnostic system consists of two digital oscilloscopes (TiePie Handyscope HS4) and six pressure transducers (PCB model 113A24) which measure the incident shock wave velocity at five locations separated by known distances, with the shock velocity extrapolated to the endwall. This extrapolated velocity was used to calculate the conditions, T_5 and p_5, behind the reflected shock wave using the CHEMKIN II [72]. The pressure at the endwall was monitored using a pressure transducer (Kistler 603B) and the ignition delay time was defined as the interval between the pressure rise due to the arrival of the incident shock wave at the endwall and the subsequent maximum rate of pressure rise, as shown in Figure 1(b).

2.3. Uncertainties related to the shock-tube experiments

There are several uncertainties associated with ignition delay times measured in shock-tube experiments. The more representative systematic errors are related to the mixture preparation, position of pressure and chemiluminescence devices, formation of boundary layer and optical access of the chemiluminescence sensor to the region of test.

2.3.1. Liquid GSBR1 mixture and reactive mixture preparation

Liquid mixtures of GSBR1 were prepared by volume (see Table 1 for compounds and percentages) and manually blended and stirred in the liquid phase for 30 min. As the surrogate fuel is a liquid at room temperature, the reactive test mixtures were prepared by a direct injection method. The mixing tanks were evacuated to 0.1 mbar and heated to 70°C. Thereafter, the fuel was injected using a gas-tight syringe, and its partial pressure was measured using a pressure transducer and digital readout. After injection of the liquid blend into the mixing vessel, the surrogate begins to evaporate. Around 90 minutes later, the pressure inside the vessel is measured and compared to the value calculated theoretically using Dalton's law, taking into account all of the compounds in the mixture of the

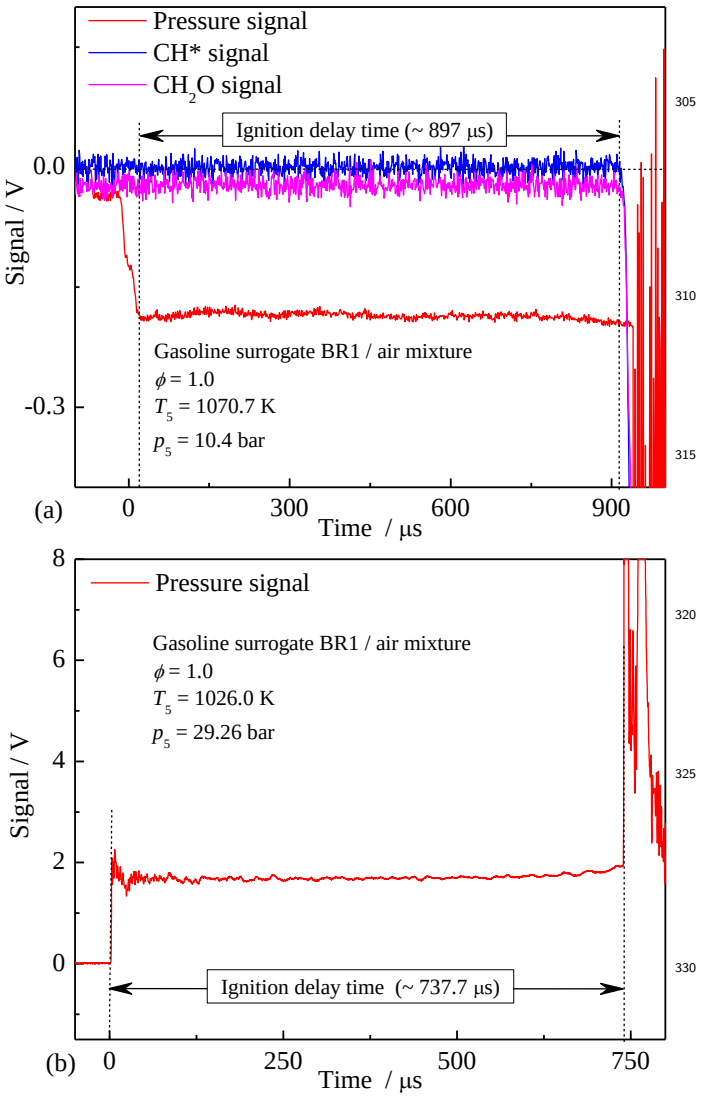

Figure 1: Ignition delay time definition at (a) HPST at IVG/UDE, (b) HPST at C3/NUIG

gasoline surrogates. In this work, there was no difference between the measured and calculated values of pressure after injection of the mixture into the mixing vessels at both IVG/UDE and C3/NUIG. This confirms that there was complete evaporation of the liquid mixture. In addition, the vapor pressure values of the compounds in the mixture must be taken into account. The vapor pressure must be above the required partial pressure of a particular compound. After complete evaporation of the liquid mixture, the vessel is then manometrically filled with synthetic air (21% O_2 and 79% N_2), until the pressure reaches the calculated value of p_{vessel} (for a set of experiments with constant stoichiometry, ϕ).

For each experiment, the test section of the HPST was carefully filled (manometrically) to a target p_1 in order to reach the desired condition of p_5 and T_5 after incident and reflected shock waves [35, 65]. Both mixture vessels are stirred magnetically (at C3/NUIG) or mechanically (at IVG/UDE), which: (a) ensures the homogenization of the reactive mixture and, (b) helps to reduce the possibility of stratification due to the density difference among the mixture components. The pressure transducers have an accuracy of 0.5% FS (full span), which results in an estimated error of about ±0.9% in the equivalence ratio of the mixture, ϕ.

2.3.2. Shock speeds measurements

In both devices the incident shock wave velocities were determined using piezoelectric pressure transducers close to the endwall of the test section, with shock attenuations of 0.7%/m to 2.5%/m. The measured shock velocities were then compared to the initially estimated values of the incident shock waves, with differences of about ±0.3% being observed. Thereafter, the reflected shock conditions were determined according to standard one-dimensional shock relations. Using the SHOCK module in CHEMKIN II [72], uncertainties of about ±0.3% in the incident wave speed yielded variations in the calculated T_5 of about ±7 K, and variations in the calculated ignition delay time of about ±7.5%. This is in agreement with the experimental uncertainties (temperature and ignition delay time) reported in the literature [35, 73, 74]. In this work, the estimated uncertainties in ignition delay times are in the range of ±7.5% to ±11%.

2.3.3. Boundary layer effects in shock tubes

In shock tube experiments there are several non-ideal effects that influence the measurement of ignition delay time. When modeling IDT in shock tubes, perfectly homogeneous reactor conditions (zeroth order approximation model) are used and then, the numerical results are compared to the measurements [35, 65]. The simulation also assumes that behind the shock wave the spatial and temporal conditions are uniform, i.e., the incident and reflected shock waves travel through the test gas and leave it unperturbed. In a real shock-heated gas there is the formation of a boundary layer at the tube wall, that grows with time given the propagation of the shock wave and the movement of the contact surface [35, 65, 75]. Observed effects of boundary layer formation and growth behind the incident shock wave include a gradual increase in temperature and pressure in the core of the flow (T_2 and p_2). When the shock wave returns as a reflected shock, it sets the temperature and pressure (T_5 and p_5) to values higher than those calculated initially using the Rankine-Hugoniot relations. Also, the displacement of the reflected shock wave also creates a boundary layer behind it, affecting the temperature and pressure (T_5 and p_5). Petersen and Hanson [76] proposed a methodology to evaluate this source of systematic error in high-pressure shock tubes, with a relation between the relative change of T_5 with reflected shock test time ($\mathrm{d}T^*/\mathrm{d}\tau_{\text{ing}}$). Equation 2 presents this relative change on temperature T_5 for larger diameter shock tubes

(∼15 cm).

$$\frac{dT^*}{d\tau_{\text{ing}}} \approx 10 \text{ s}^{-1} \quad (2)$$

For shock tube diameters smaller than 10 cm the relative change ($T^* = \Delta T_5 \ / \ T_{5-\text{initial}}$) increases to values of 20 s^{-1} to 30 s^{-1}. Assuming that boundary layer effects have a major systematic error on temperature, and for shock tube diameters of 9 cm (IVG/UDE) and 6.3 cm (C3/NUIG). In this work values of 20 s^{-1} and 26 s^{-1} (respectively) were assumed for the determination of uncertainties in both HPSTs. Tables 2 and 4 show the estimated values of ΔT_5 for all of the IDTs measured in this work.

2.4. Experimental conditions

Experiments were carried out covering a wide range of operation conditions, i.e., temperatures, pressures, and equivalence ratios as found in internal combustion engines (SI and HCCI engines). Table 2 summarizes all of the experimental conditions studied in this work. Information related to the absolute mole fraction of each component for all equivalence ratios can be found as supplementary material.

Table 2: Experimental conditions for IDT measurements in this work

Mixture	GSBR1 in synthetic air
Pressures, (bar)	10 - 30
Stoichiometries, ϕ	0.35 - 0.7 - 1.00 - 1.30
Temperature range, (K)	749 to 1204

GSBR1 compounds and volumetric percentage (vol.%): Ethanol/*n*-Heptane/*i*-Octane/1-Hexene/Methylcyclohexane/Toluene 27.0/11.5/30.0/5.0/7.0/19.5 (vol.%)
Synthetic air (21% O_2 and 79% N_2)

3. Numerical approach

Numerical simulations of the IDT experiments were conducted using the CANTERA software, version 2.4.0, [77]. Simulations were performed assuming an isochoric – adiabatic homogeneous reactor. Numerically, the thermal ignition was defined as the time of maximum OH concentration along the simulation process [35, 49, 78].

3.1. Reduced chemical kinetics model

In this work, a reduced kinetics model is proposed, based on a detailed mechanism from the CRECK modeling group at Politecnico di Milano (POLIMI TOT 1412 kinetics mechanism, Version 1412, December 2014) [79]. The POLIMI TOT 1412 model was constructed in a hierarchical way by adding to a base core-kinetics model the chemical sub-mechanisms for other species with molecular mass larger than those of the core kinetics. The development and validation of this mechanism employed a vast amount of experimental data of laminar flame speeds of hydrocarbons and oxygenated fuels including C_0 to C_4 species, reference fuels, alkanes (*n*-heptane, *iso*-octane, *n*-decane, *n*-dodecane), cyclo-alkanes (cyclohexane and methyl-cyclohexane), aromatics (benzene, toluene, xylene and ethylbenzene), oxygenated fuels (C_3H_6O isomers, dimethyl ether and ethyl tertiary butyl ether), and methyl esters up to methyl decanoate [79]. As a result, the POLIMI TOT 1412 mechanism has 17848 elementary reactions among 451 species. The fine agreement observed across the entire range of conditions investigated was used to confirm the reliability and validity of the kinetics model. The mechanism was also validated by comparing predicted and calculated ignition delay time in shock tubes and concentration profiles of the isomers of butanol (*n*-butanol - *n*-C_4H_9OH), *sec*-butanol - *sec*-C_4H_9OH), *iso*-butanol - *iso*-C_4H_9OH, and *tert*-butanol - *tert*-C_4H_9OH) measured in batch reactors, plug-flow reactors and in a jet-stirred reactor [80, 81].

Even though CANTERA can reasonably handle such extensive mechanisms for ignition delay time simulations, it is unwieldy to compute phenomena like laminar flame speed. In order to reduce the detailed mechanism, a script, native to CANTERA, was employed. In summary the script runs an IDT simulation and, at each time step, ranks the elementary reactions according to their relative net reaction rate. In order to obtain an adequate reduced mechanism the simplification procedure was carried out as follows: (1) a set of simulation conditions was used as reference; equivalence ratios $\phi = 0.35$, 0.70, 1.00 and 1.30, temperatures of $T = 800$ K and 1100 K, and pressures of $p =$ 10 bar and 30 bar. This set of conditions results in 16 simulations for each mixture to be compared (full mechanism against reduced mechanism). (2) all IDT cases were computed using a constant volume, adiabatic, homogeneous reactor model using the full mechanism, thus defining a reference IDT to be compared to the IDT obtained from the reduced kinetics model. (3) comparisons were performed testing the predictions of the reduced model for each of the six pure components of the GSBR1 surrogate as well as the complete blend, therefore resulting in 224 simulations (112 each for both the full and reduced mechanisms). (4) a maximum relative difference (Equation 3) of 0.1 (%) was defined in order to set the stop criteria for reaction number reduction. On each case the top 4000 reactions were selected, with the final reduced, yet still quite detailed, mechanism comprising 4885 reactions among 318 chemical species.

$$\text{Rel}_{\text{diff}}(\%) = \left[\frac{\text{IDT}_{\text{full\_mech}} - \text{IDT}_{\text{red\_mech}}}{\text{IDT}_{\text{full\_mech}}}\right] \times 100 \quad (3)$$

Figure 2 shows the relative difference (Equation 3) obtained in all simulations performed along the reduction process. It is important to note that the reduction process was performed by comparing numerical to numerical data, while no experimental validation was performed for mechanism reduction.

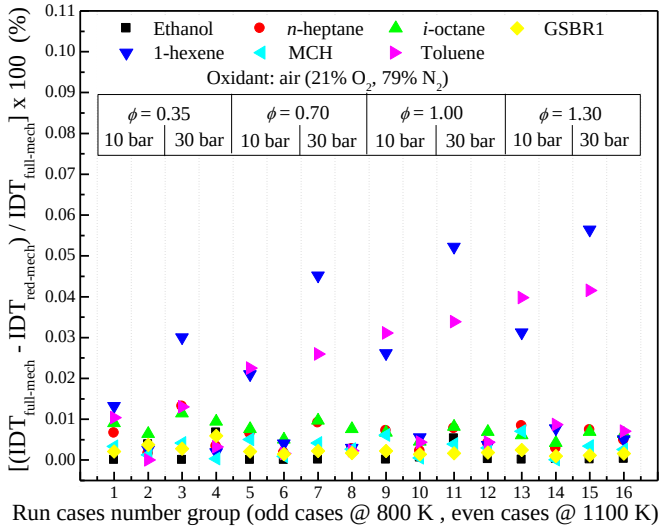

Figure 2: Relative difference of predicted ignition delay times (IDT) using the full model [79] and the reduced model proposed in this work.

It can be observed that the relative difference defined in Equation 3, for all of the mixtures numerically tested was below 0.056% for all conditions of ϕ, T and p investigated. Figure 2 shows that moving in the direction of rich mixtures, the relative difference in IDT predictions increases for toluene and 1-hexene. For the others fuels tested, the relative difference was quite constant and below 0.02%. The threshold of 0.1 (%), defined as stop criteria for reaction number reduction in Equation 3, yields a reduced kinetics model with 4885 elementary reactions among 318 species. Table 3 presents a comparison of both kinetics mechanisms as well as the average time for the simulations. The reduced mechanism (in CANTERA format) as well as the glossary of species are available as Supplementary Material.

Table 3: Main characteristics of the detailed kinetics model [79] and the reduced kinetics model proposed in this work.

Mechanism	Detailed [79]	Reduced
Elements	5	5
Species	451	326
Reactions	17848	4885
Average time per run*	50 s	12 s

* Constant volume homogeneous reactor simulation in CANTERA [77] - Computation performed in a personal computer Intel Core i7-5500U CPU @ 2.40 GHz

4. Results and discussion

4.1. Ignition delay time measurements

The two facilities used covered a wide range of pressure, temperature and stoichiometry in the experiments using the GSBR1. Tables 4 and 5 list all the experimental data measured using both HPSTs. Figure 3(a) shows the data trend for experiments at IVG/UDE. Figure 3(b) shows the data trend for the experiments at C3/NUIG. Figure 3(c) shows the experimental data from both HPSTs. Several observations can be made at this point. The IDT data trends do not show any NTC behavior, indicating that the volumetric percentage of n-paraffins (11.5% n-heptane) does not impact the overall reaction rate at low temperatures ($T < 950$ K). Figure 3(c) shows the good agreement between the data recorded using both facilities, with measurements in the range of 1200 K $< T <$ 980 K overlapping for the pressures and equivalence ratios investigated.

The data can be fitted to an equation of the form of Equation 1 using multiple linear regression analysis with $\ln(\tau_{ing})$ as the dependent variable and $(1000/T_5)$, $\ln(p)$ and $\ln(\phi)$ as independent variables identified the value of $x = 0.72$ and $y = 0.62$, as well as a global activation energy of ≈109 kJ/mol. Equation 4 shows the fitted expression in the modified Arrhenius from.

$$\tau_{ign}/\mu s = 10^{(-1.66\pm0.18)} \exp\left(\frac{109\pm3.40\ \mathrm{kJ/mol}}{RT}\right) (p/\mathrm{bar})^{(-0.72\pm0.06)}\ \phi^{(-0.62\pm0.06)} \quad (4)$$

The coefficient of determination of the multiple linear regression was $R^2 \approx 0.95$ for the experimental data shown in Tables 4 and 5, from both the facilities. The fitting was determined for the experimental data using temperatures above 900 K, considering the pressures and stoichiometries from Table 2.

It can be clearly seen that the T-dependence of autoignition delay times flatten when moving from the high- to low-temperature regime and that the global activation energy drops for temperatures below 900 K. Similarly, these changes in the τ_{ing} slope are also observed in many experimental results in the literature for different fuels [21, 35, 49, 82, 78, 83, 84].

4.2. Numerical predictions using the reduced kinetics model

Figure 4 shows the numerical prediction of all of the experimental data reported in Tables 4 and 5.

Several observations can be made from this comparison. The first is that the reduced kinetics model reproduced the experimental results comparatively well in the high to middle temperature range investigated in this work (1200 K $\lesssim T \lesssim$ 900 K), and the accuracy increases as equivalence ratio increases. Also, the proposed reduced model reproduces the bend in the experimental data for p = 30 bar and $\phi = 1.0$ at low temperatures, while for leaner mixtures and low pressures the reduced model is able to qualitatively follow the experiments.

4.2.1. Brute-force sensitivity analysis on IDT

In order to better understand the reduced ability to predict the ignition delay times at low temperatures, a brute force sensitivity analysis on IDT was performed.

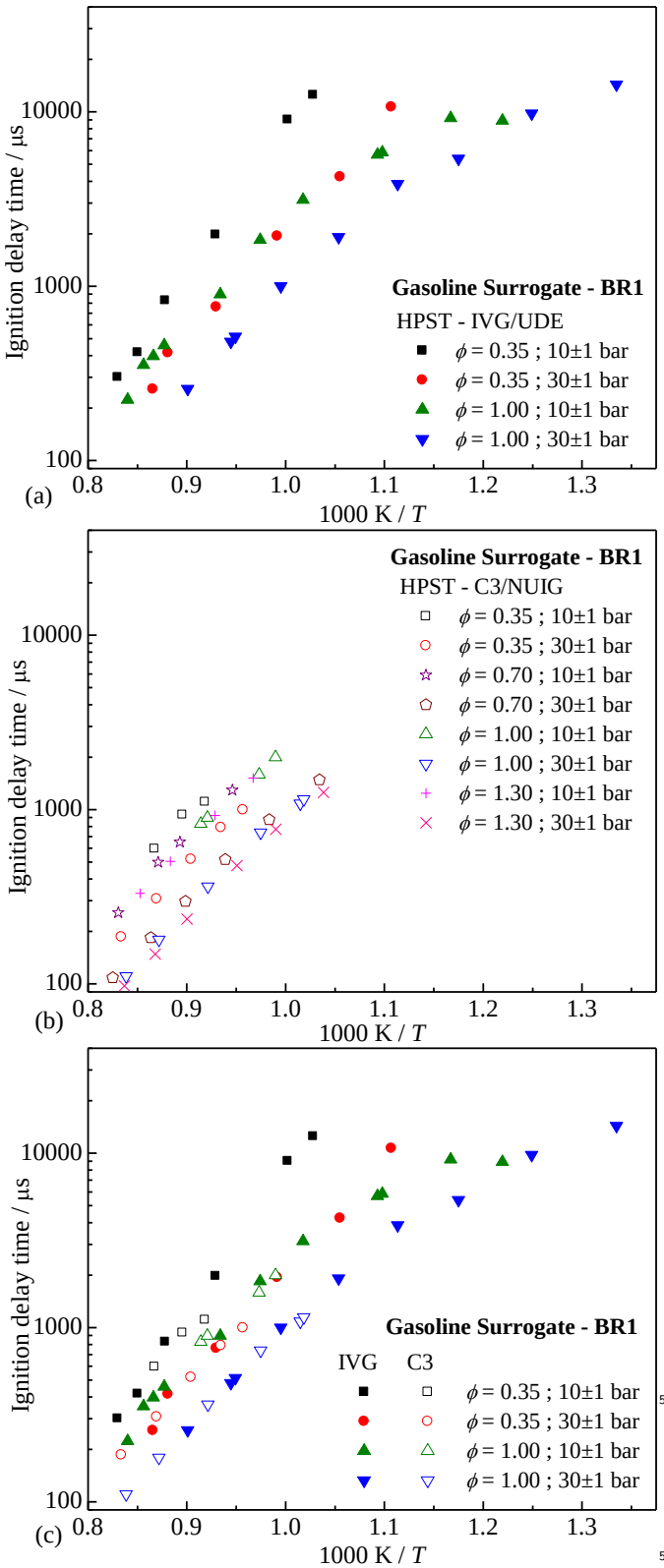

Figure 3: Experimental IDT data from (a) IVG/UDE, (b) C3/NUIG and (c) IVG/UDE and C3/NUIG at the same experimental conditions of pressure and equivalence ratio

Simulations were performed for twenty-four sets of conditions: temperatures of 750 K, 900 K and 1050 K, stoichiometries were set at $\phi = 0.35$ and $\phi = 1.00$, and two points of pressures where analyzed (10 and 30 bar), with the perturbation being generated by multiplying the reaction rate (k) of each reaction of the reduced model by 0.5 and 2.0, and then calculating the IDT for each perturbation. Each brute force sensitivity analysis, programmed in CANTERA [77] took 47.5 hours running in a HP - Workstation Intel Xeon E5420 CPU @ 2.50 GHz.

Table 4: Gasoline surrogate BR1 ignition delay time measurements at IVG/UDE

ϕ	T_5 (K)	$\pm\Delta T_5$ (K)	p_5 (bar)	τ_{ing} (μs)
0.35	1205.1	0.7	10.0	301.3
0.35	1176.4	1.0	10.5	417.2
0.35	1139.2	1.9	10.8	829.9
0.35	1076.5	4.3	10.5	1975.7
0.35	997.9	18.0	9.9	9028.2
0.35	973.0	24.3	10.6	12495.9
0.35	907.2	***	10.2	N.I[a]
0.35	1155.2	0.6	30.2	257.3
0.35	1135.1	0.9	32.1	415.3
0.35	1075.5	1.6	31.5	759.9
0.35	1008.4	3.9	30.5	1938.2
0.35	947.6	8.0	29.6	4243.1
0.35	903.4	19.3	30.2	10674.4
0.35	831.1	***	33.0	N.I[a]
0.35	750.4	***	30.0	N.I[a]
1.00	1190.3	0.5	10.7	223.6
1.00	1167.8	0.8	9.3	353.7
1.00	1154.4	0.9	9.1	397.1
1.00	1140.2	1.0	10.8	458.0
1.00	1070.7	1.9	10.4	897.0
1.00	1026.6	3.8	10.6	1846.8
1.00	982.6	6.2	10.8	3130.6
1.00	915.0	10.4	10.4	5683.3
1.00	910.8	10.7	10.2	5865.3
1.00	856.9	15.8	10.2	9198.6
1.00	820.0	14.6	10.6	8908.7
1.00	767.9	***	10.6	N.I[a]
1.00	1110.1	0.6	30.4	257.8
1.00	1058.8	1.0	30.4	481.0
1.00	1053.5	1.1	30.0	513.0
1.00	1004.8	2.0	30.1	998.9
1.00	949.1	3.6	29.7	1914.4
1.00	898.2	6.9	29.7	3866.0
1.00	851.1	9.2	30.0	5394.8
1.00	800.6	15.6	29.9	9764.7
1.00	749.1	21.5	29.8	14344.3

[a]N-I = no ignition within the test time

Equation 6 shows the sensitivity criteria adopted in this work for the brute force analysis. Therefore, if the sensitivity (S) is zero, the perturbed reaction has no influence on IDT, if the sensitivity (S) is higher than zero, the perturbed reaction increases the IDT (positive influence) and conversely it reduces the IDT (negative influence).

$$S_{(\text{sensitivity})} = \frac{\tau_{\text{with perturbation}}}{\tau_{\text{without perturbation}}} - 1 \qquad (5)$$

Table 5: Gasoline surrogate BR1 ignition delay time measurements at C3/NUIG

ϕ	T_5 (K)	$\pm\Delta T_5$ (K)	p_5 (bar)	τ_{ing} (μs)
0.35	1152.3	1.8	9.7	596.5
0.35	1116.7	2.7	9.7	935.7
0.35	1089.0	3.1	9.7	1109.0
0.35	1199.4	0.6	29.7	186.0
0.35	1150.0	0.9	30.1	307.3
0.35	1105.8	1.5	30.4	519.0
0.35	1070.0	2.2	30.7	788.7
0.35	1045.0	2.7	30.8	995.3
0.70	1204.0	0.8	9.6	256.4
0.70	1148.0	1.5	9.9	497.7
0.70	1120.0	1.9	10.3	650.5
0.70	1057.0	3.6	10.0	1293.0
0.70	1212.0	0.3	30.3	108.6
0.70	1185.0	0.6	30.1	184.4
0.70	1112.7	0.9	30.4	297.8
0.70	1065.0	1.4	30.6	517.0
0.70	1017.0	2.3	30.9	873.8
0.70	967.0	3.7	30.9	1482.0
1.00	1094.0	2.4	9.3	830.0
1.00	1086.0	2.5	9.7	897.0
1.00	1027.5	4.2	9.3	1589.0
1.00	1010.2	5.3	9.4	2000.0
1.00	1192.5	0.3	29.1	110.6
1.00	1147.0	0.5	29.8	179.2
1.00	1085.5	1.0	29.7	361.4
1.00	1026.0	2.0	29.3	737.7
1.00	985.3	2.8	29.6	1081.0
1.00	981.9	2.9	30.1	1147.0
1.30	1173.0	1.0	9.4	331.0
1.30	1132.0	1.5	9.5	504.7
1.30	1077.0	2.6	9.4	925.5
1.30	1034.0	4.1	9.5	1517.0
1.30	1195.0	0.3	29.3	97.5
1.30	1152.0	0.4	29.8	148.5
1.30	1111.0	0.7	30.3	235.5
1.30	1051.8	1.3	29.7	476.7
1.30	1010.0	2.0	30.3	770.3
1.30	963.0	3.1	30.7	1252.0

Reactions with sensitivities below the threshold were then ignored for plotting. Figures 5 and 6 shows the classical bars diagram for perturbation of 0.5 and 2.0 respectively.

The analysis pointed out the following twenty-two reactions as the most influencing of the reduced kinetics model (4885 reactions), taking the threshold value of 0.5 % change (absolute) on the IDT:

$$2OH(+M) \Leftrightarrow H_2O_2(+M) \quad \text{(R.1)}$$

$$nC_7H_{16}+OH \Rightarrow H_2O + nC_7H_{15} \quad \text{(R.2)}$$

$$nC_7-QOOH + O_2 \Rightarrow nC_7-OOQOOH \quad \text{(R.3)}$$

$$nC_7-OOQOOH \Rightarrow nC_7-OQOOH + OH \quad \text{(R.4)}$$

$$C_2H_5OH + OH \Rightarrow CH_3CHOH + H_2O \quad \text{(R.5)}$$

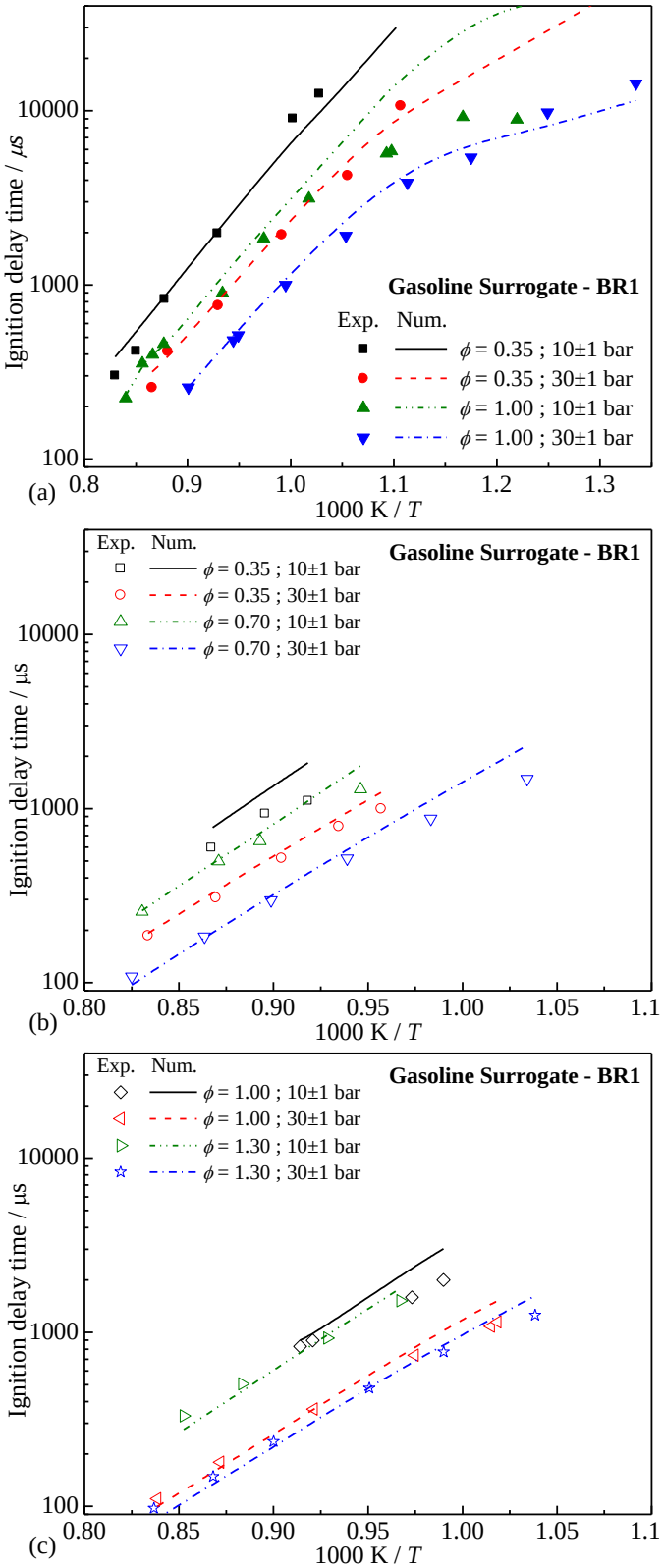

Figure 4: Experimental data (symbols) and numerical (lines) IDT prediction using the reduced model proposed in this work (a) HPST - IVG/UDE, (b) and (c) HPST - C3/NUIG

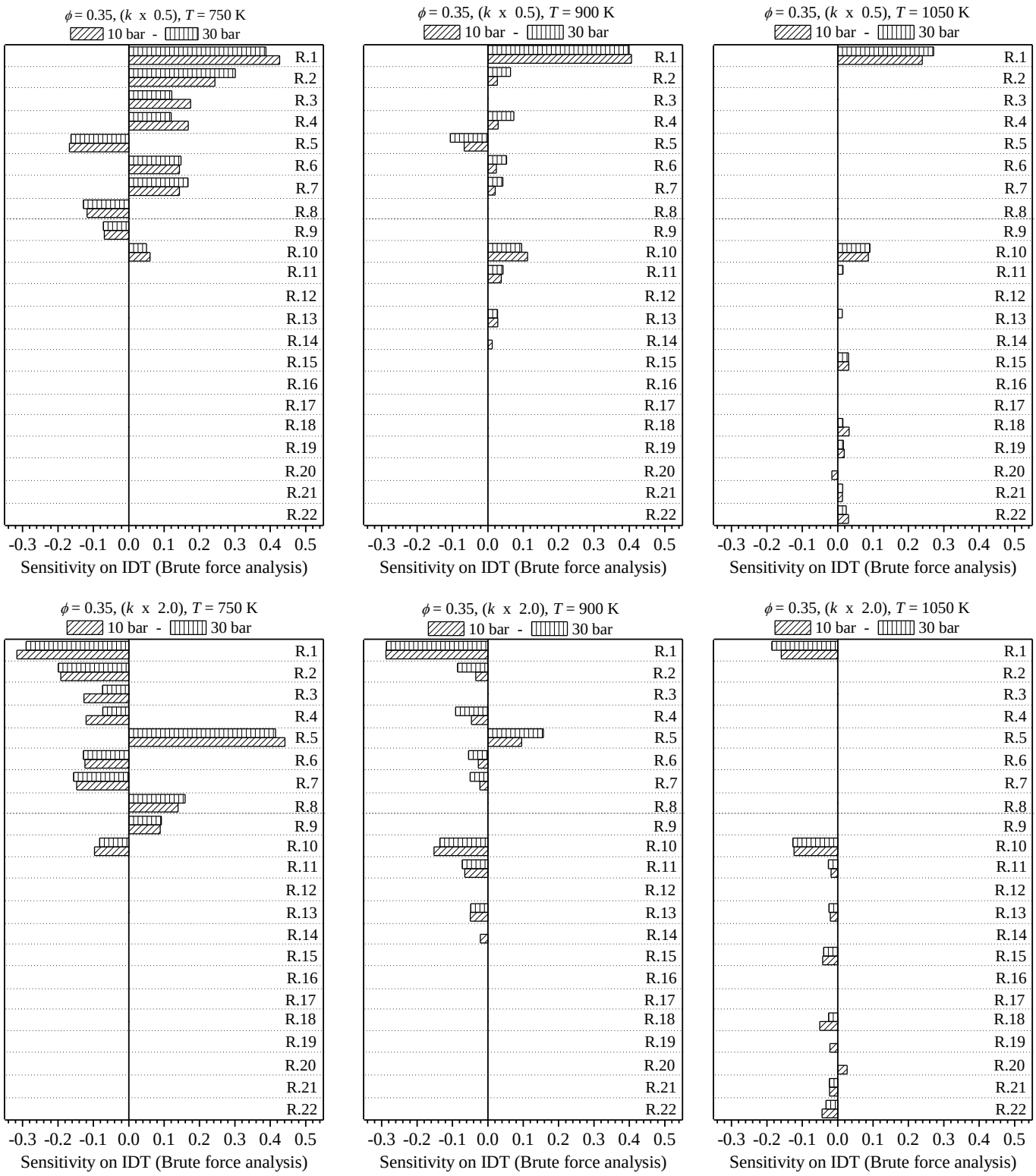

Figure 5: Brute force sensitivity on IDT for GSBR1 / air mixtures at pressures of 10 and 30 bar, $\phi = 0.35$, at temperatures of 750 K, 900 K and 1050 K, and perturbation of $k \times 0.5$ and $k \times 2.0$

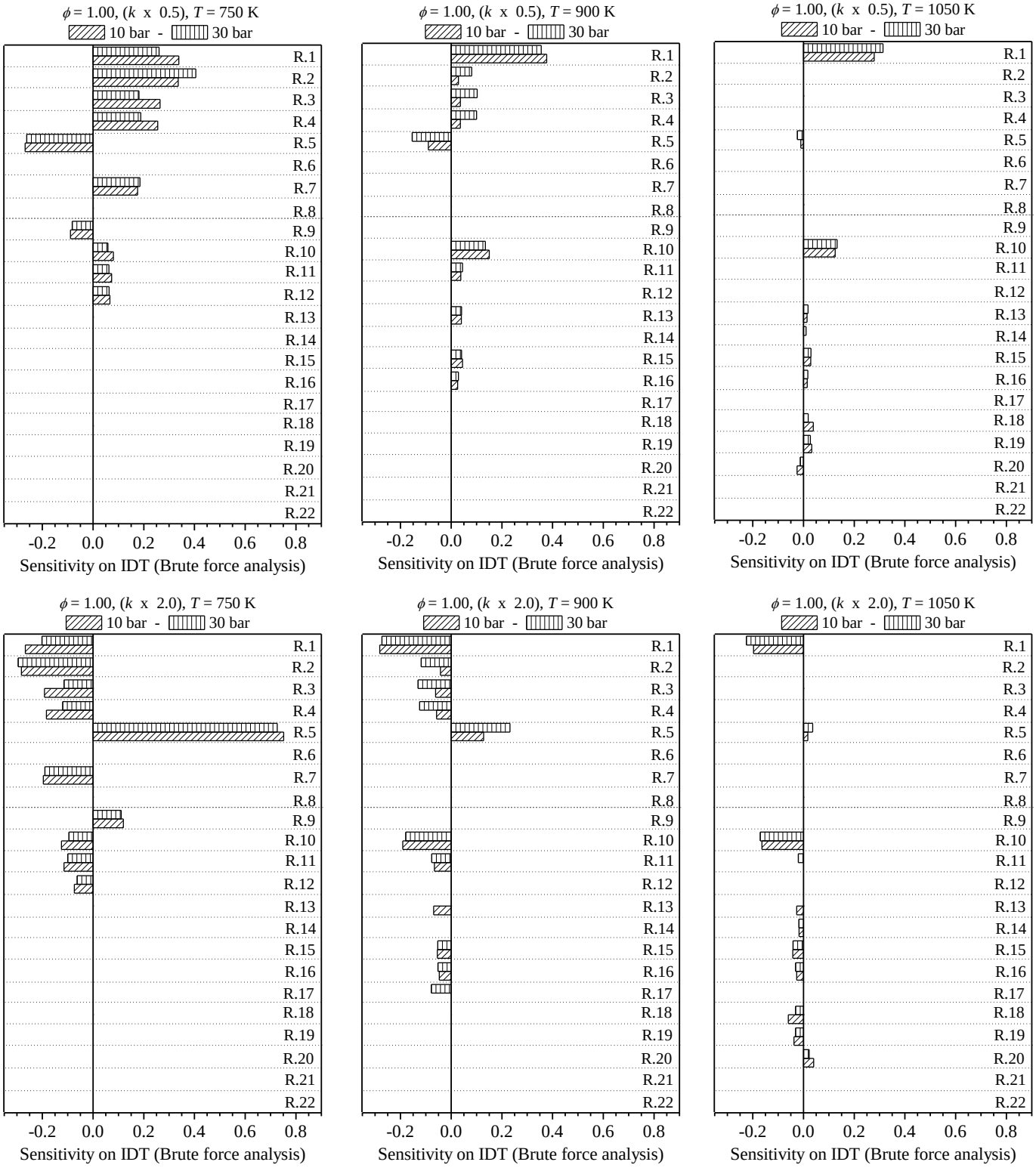

Figure 6: Brute force sensitivity on IDT for GSBR1 / air mixtures at pressures of 10 and 30 bar, $\phi = 1.00$, at temperatures of 750 K, 900 K and 1050 K, and perturbation of $k \times 0.5$ and $k \times 2.0$

$$iC_8H_{17}{-}OO \Rightarrow iC_8{-}QOOH \quad \text{(R.6)}$$

$$iC_8H_{18}{+}OH \Rightarrow H_2O + iC_8H_{17} \quad \text{(R.7)}$$

$$iC_8H_{17}{-}OO \Rightarrow iC_8T - QOOH \quad \text{(R.8)}$$

$$iC_8{-}OOQOOH \Rightarrow \tfrac{21}{100}C_2H_5CHO + CH_2O + CH_3COCH_3 + \tfrac{79}{100}iC_3H_7CHO + \tfrac{21}{400}iC_4H_8 + OH \quad \text{(R.9)}$$

$$C_2H_5OH + HO_2 \Rightarrow \frac{1}{3}C_2H_4OH + \frac{2}{3}CH_3CHOH + H_2O_2 \quad \text{(R.10)}$$

$$C_7H_8{+}OH \Rightarrow C_7H_7{+}H_2O \quad \text{(R.11)}$$

$$MCYC_6{+}OH \Rightarrow H_2O + RMCYC_6 \quad \text{(R.12)}$$

$$C_7H_8{+}HO_2 \Rightarrow C_7H_7{+}H_2O_2 \quad \text{(R.13)}$$

$$nC_6H_{12}{+}OH \Rightarrow \frac{1}{2}C_2H_3{+}\frac{1}{2}C_3H_6{+}\frac{1}{2}CH_2CHCH_2{+}H_2O{+}\frac{1}{2}nC_4H_8 \quad \text{(R.14)}$$

$$C_7H_7{+}O_2 \Rightarrow C_6H_5{+}CH_2O + O \quad \text{(R.15)}$$

$$HO_2{+}iC_8H_{18} \Rightarrow H_2O_2{+}iC_8H_{17} \quad \text{(R.16)}$$

$$iC_8{-}OOQOOH \Rightarrow iC_8{-}OQOOH + OH \quad \text{(R.17)}$$

$$iC_8H_{18} \Rightarrow \frac{1}{5}iC_3H_7{+}\frac{4}{5}iC_4H_9P{+}\frac{4}{5}iC_4H_9T{+}\frac{1}{5}neoC_5H_{11} \quad \text{(R.18)}$$

$$C_7H_7{+}HO_2 \Rightarrow C_6H_5{+}CH_2O + OH \quad \text{(R.19)}$$

$$C_7H_8{+}O_2 \Leftrightarrow C_7H_7{+}HO_2 \quad \text{(R.20)}$$

$$C_2H_5OH + OH \Rightarrow C_2H_4OH + H_2O \quad \text{(R.21)}$$

$$C_2H_4{+}OH \Leftrightarrow C_2H_3{+}H_2O \quad \text{(R.22)}$$

As expected, the predominant chain branching reaction of the H_2/O_2 system, $2OH(+M) \Leftrightarrow H_2O_2(+M)$, is important in the sensitivity analysis for all conditions, (R.1). The Arrhenius parameters of this reaction have been well defined by many research groups. At 750 K the reaction (R.5), between ethanol and $\dot{O}H$, $C_2H_5OH + \dot{O}H \Rightarrow CH_3\dot{C}HOH + H_2\dot{O}$, strongly affects the IDT, especially for $k \times 2.0$. Another important reaction with ethanol is (R.10), $C_2H_5OH + H\dot{O}_2 \Rightarrow \frac{1}{3}\dot{C}_2H_4OH + \frac{2}{3}CH_3\dot{C}HOH + H_2\dot{O}_2$, which increases IDT for $k \times 0.5$. Besides these reactions with ethanol, the addition of hydroperoxyl heptyl radicals to O_2 (R.3) and the subsequent formation of $\dot{O}H$ radicals (R.4) produced for the formation and decomposition of carbonyl hydroperoxide species are also important at low temperatures. For *iso*-octane, some internal isomerizations (R.6) increase reactivity while others (R.8) decrease it.

At 900 and 1050 K, (R.1) and (R.5) also present significant sensitivity. The other noteworthy reactions at these temperatures are those involving toluene and benzyl radical ((R.11), (R.13), (R.15), (R.19), (R.20)), mostly decreasing reactivity. For fuel-lean mixture, $\phi = 0.35$, and 1050 K, H-atom abstraction by $\dot{O}H$ from ethanol, (R.21), and ethylene, (R.22), also affected IDT predictions.

Figure 5 (lean composition) shows that reactions (R.2) to (R.9) have a relatively strong effect on IDTs at low temperatures for fuel-lean conditions. As the temperature increases the effect on IDT decreases, for 1050 K the perturbation $k \times 0.5$ has no effect on the IDT, quite the same trend can be observed for perturbation $k \times 2.0$. Reaction (R.10) shows a constant effect on IDT at low and high temperatures. From Figure 5 (stoichiometric composition) the effect of rate of perturbation $k \times 0.5$ of reactions (R.2) to (R.9) are similar to the fuel-lean condition, at high temperatures the effect on IDT is negligible, as well as for the perturbation $k \times 2.0$.

4.3. Comparison to IDT / AKI data available at literature

As mentioned in the Introduction, IDTs for several surrogates and real fuels are available in the literature. In this work published data were compared taking into account the surrogate formulation in terms of oxygenates percentage and / or the anti-knock index of the fuel / mixture of surrogates. Figure 7 shows the comparison of the measured IDT in this work to the IDT measurements from [85], [86] and [41]. All data was normalized to 30 bar and $\phi = 1.00$ using $1/p$ and $1/\phi$.

Figure 7(a) shows the strong NTC behavior of fuels FACE A, C, F and G at temperatures below 915 K. The GSBR1 mixture proposed in this work does not show any NTC behavior for the experimental conditions investigated. Analyzing the composition of each fuel, the GSBR1 mixture contains a low concentration of *n*-paraffins, and a high concentration of alcohol and reasonable quantities of aromatic and *iso*-paraffin, as shown in Table 1. It should be noted that FACE A, C and F fuels have low concentrations of aromatics (0.3 mol.%, 4.4 mol.% and 8.4 mol.% respectively) as well as intermediate to high concentrations of *n*-alkanes (13.2 mol.%, 28.6 mol.% and 4.8 mol.% respectively), but they have no oxygenates. These features may be responsible for the NTC behavior of these fuels. For FACE G fuel, the aromatic content (31.8 mol.%) is higher when compared to the others fuels. However, its *iso*-paraffins content is lower (38.3 mol.%), has no oxygenates and in the same way as for the FACE A, C and F fuels, these features may be the responsible for the NTC behavior of FACE G fuel. Fuels FUEL C and D, from [85], have relatively high AKI as shown in Figure 7(a), and only FUEL D includes oxygenates in the composition (8.0 mass.%). Experimental data of IDT with its related AKI information, for mixtures containing oxygenates is scarce at the literature.

Figure 7(b) shows the scaled (to 30 bar) IDT data at temperatures below those of the NTC region. It can be observed that the data can be fitted to a modified Arrhenius plot, in the form of Equation 1. Using a multiple linear regression analysis with $\ln(\tau_{30})$ as the dependent variable, $(1000/T_5)$ and $\ln(\text{AKI})$ as independent variables identified a value of $x = -1.11$ as the AKI exponent dependency as

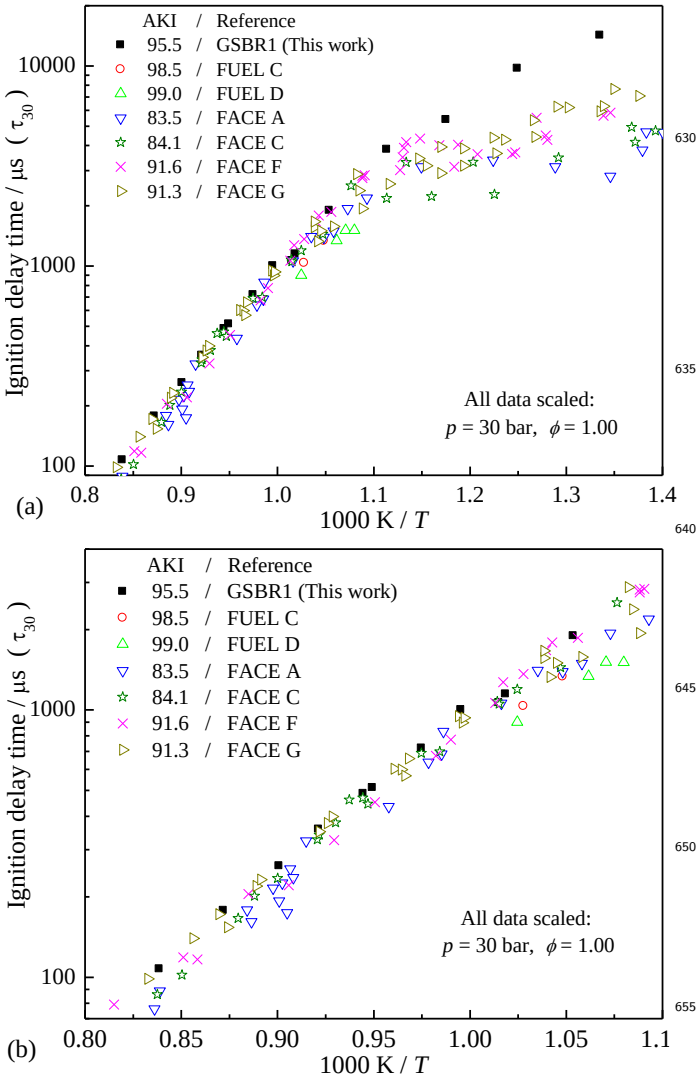

Figure 7: Scaled ignition delay times to 30 bar (τ_{30}) and stoichiometric composition ($\phi = 1.00$). References of experimental data: FUEL C and FUEL D fuels from [85], FACE A and FACE C fuels from [86], and FACE F and FACE G fuels from [41].

well as a global activation energy of ≈109 kJ/mol. Equation 6 shows the fitted expression in the modified Arrhenius from.

$$\tau_{30}/\mu s = 10^{(-4.92\pm0.47)} \exp\left(\frac{109\pm1.32 kJ/mol}{RT}\right) \times (AKI)^{(1.11\pm0.24)} \quad (6)$$

The coefficient of determination of the multiple linear regression was $R^2 \approx 0.99$ for the experimental data shown in Figure 7(b), covering the temperature range 1225 K $\lesssim T \lesssim$ 915 K, scaled IDT to 30 bar (τ_{30}) and $\phi = 1.00$, and the anti-knock index range 95.5 $\lesssim$ AKI $\lesssim$ 83.5. Because of the low number of experiments at 30 bar recorded for FUEL C and D, the six experimental points of those fuels where removed for the multiple linear regression of Eq. 6.

Below 915 K all the fuels holding low content of aromatics and *iso*-paraffins as well as representative quantity of *n*-paraffins shows NTC behavior, indicating that for low temperatures the IDT–AKI relationship is strong dependent on the fuel composition.

5. Conclusions

In this work, a novel, six-component, high performance gasoline surrogate (GSBR1) is proposed and investigated experimentally and numerically to determine its thermal ignition. The proposed surrogate is composed of ethanol, *n*-heptane, *i*-octane, 1-hexene, methylcyclohexane, and toluene (AL-P-I-O-N-A) with 27% of ethanol. Experiments were carried out at C3/NUIG and IVG/UDE using high pressure shock tubes with different operation characteristics (double diaphragm at C3/NUIG and single diaphragm at IVG/UDE). The data show good agreement with one another for results in the overlap temperature and pressure ranges from both shock tubes, as shown in Fig. 3(c).

A modified Arrhenius equation was developed using multiple linear regression for experiments with temperatures higher than 900 K. Pressure and equivalence ratio dependence coefficients of 0.72 and 0.62 (respectively) were obtained from the fit, as well as a global activation energy of ≈109 kJ/mol.

A simplistic approach to mechanism reduction, based on the elimination of reactions with no relevant rate of progress was used in order to reduce an extensive detailed kinetic model (hierarchically constructed with more than 17800 reactions). The reduced, though still detailed, kinetic model with 4885 elementary reactions among 326 chemical species was used for numerical simulations and its predictions were compared with the experimental data obtained herein. The reduced kinetics model reproduced relatively well the experimental results in the high temperature range, and the accuracy increases as the mixture stoichiometry increases. Moreover, the proposed reduced model reproduces the bend of the experimental data for p = 30 bar and $\phi = 1.00$ at low temperatures.

It was observed that for low temperatures the proposed reduced kinetics model agreement with data was only qualitative. In order to understand the likely cause of this discrepancy, a brute force sensitivity analysis on IDT was performed, elucidating of this form the more influencing reactions. Work is currently continuing on identifying the chemistry and surrogate species and H-atom abstraction species resulting from the decomposition of the surrogates, the brute force sensitivity analysis identifying the more important reactions controlling reactivity in the mechanism, to be considered for further analysis and optimization. For example, it was observed that reactions involving ethanol, *iso*-octane and toluene reacting with OH and HO_2 showed significant sensitivity for IDT, being noteworthy that these three surrogates species represent around 77 % of the GSBR1 composition.

The experimental data obtained in this study was compared to data available in the literature in terms of anti-knock index at a scaled pressure of 30 bar for the stoichiometric condition. A modified Arrhenius equation was then fitted and it elucidated an AKI dependence exponent of −1.11 for the data used in the multiple linear regression. This means that the higher the AKI, the longer is the IDT, independent of fuel composition (chemical groups). At temperatures below the NTC region, that trend should be confirmed with further investigations by compiling a sufficient volume of experimental data. At low temperatures all of the fuels with low concentrations of aromatics and *iso*-paraffins as well as appreciable quantities of *n*-paraffins shows NTC behavior, indicating that for low temperatures the IDT–AKI relationship strongly depends on the fuel composition.

Acknowledgments

The main author gratefully acknowledges the support from *Fundação Stemmer para Pesquisa, Desenvolvimento e Inovação* FEESC, the *Pró-Reitoria de Pesquisa* - PROPESQ / UFSC, the *Centro Tecnológico de Joinville* - CTJ/UFSC and the *Conselho Nacional de Desenvolvimento Científico e Tecnológico* - CNPq (Processo 454217/2017-0). The RON and MON measurements of the GSBR1 mixture performed at CENPES / PETROBRAS by A. C. B. Bontorin, A. Rouge and E. J. Oliveira. The help and support of J. Herzler, N. Schlösser, M. Baigmohammadi, N. Lokachari and S. Nagaraja are also greatly appreciated.

6. References

[1] The European Commission regulatory proposal for post-2020 CO_2 targets for cars and vans: A summary and evaluation, Technical report, International Council on Clean Transportation (2018).

[2] G. Kalghatgi, Is it really the end of internal combustion engines and petroleum in transport?, Applied Energy 225 (2018) 965 – 974. doi:10.1016/j.apenergy.2018.05.076.

[3] A. Demirbas, Biofuels securing the planet's future energy needs, Energy Conversion and Management 50 (9) (2009) 2239 – 2249. doi:10.1016/j.enconman.2009.05.010.

[4] P. Hofmann, T. Hofherr, G. Hoffmann, J.-F. Preuhs, Potential of CNG Direct Injection for Downsizing Engines, MTZ worldwide 77 (2016) 28–35. doi:doi.org/10.1007/s38313-016-0074-6.

[5] M. Canakci, Combustion characteristics of a di-hcci gasoline engine running at different boost pressures, Fuel 96 (2012) 546 – 555. doi:10.1016/j.fuel.2012.01.042.

[6] J. M. Bergthorson, M. J. Thomson, A review of the combustion and emissions properties of advanced transportation biofuels and their impact on existing and future engines, Renewable and Sustainable Energy Reviews 42 (2015) 1393–1417. doi:10.1016/j.rser.2014.10.034.

[7] Y. Putrasaria, N. Jamsrana, O. Lim, An investigation on the DME HCCI autoignition under EGR and boosted operation, Fuel 200 (2017) 447 – 457. doi:10.1016/j.fuel.2017.03.074.

[8] A. Turkcan, M. D. Altinkurt, G. Coskun, M. Canakci, Numerical and experimental investigations of the effects of the second injection timing and alcohol-gasoline fuel blends on combustion and emissions of an hcci-di engine, Fuel 219 (2018) 50 – 61. doi:10.1016/j.fuel.2018.01.061.

[9] Y. Zhou, D. Hariharan, R. Yang, S. Mamalis, B. Lawler, A predictive 0-D HCCI combustion model for ethanol, natural gas, gasoline, and primary reference fuel blends, Fuel 237 (2019) 658–675. doi:10.1016/j.fuel.2018.10.041.

[10] Z. Wang, G. Du, Z. Li, X. Wang, D. Wang, Study on the combustion characteristics of a high compression ratio hcci engine fueled with natural gas, Fuel 255 (2019) 115701. doi:10.1016/j.fuel.2019.115701.

[11] L. Xu, X.-S. Bai, C. Li, P. Tunestl, M. Tunr, X. Lu, Emission characteristics and engine performance of gasoline dici engine in the transition from hcci to ppc, Fuel 254 (2019) 115619. doi:10.1016/j.fuel.2019.115619.

[12] X. Liu, S. Kokjohn, Y. Li, H. Wang, H. Li, M. Yao, A numerical investigation of the combustion kinetics of reactivity controlled compression ignition (rcci) combustion in an optical engine, Fuel 241 (2019) 753 – 766. doi:10.1016/j.fuel.2018.12.068.

[13] Y. Putrasari, O. Lim, A study on combustion and emission of gci engines fueled with gasoline-biodiesel blends, Fuel 189 (2017) 141 – 154. doi:10.1016/j.fuel.2016.10.076.

[14] H. Bendu, S. Murugan, Homogeneous charge compression ignition (HCCI) combustion: Mixture preparation and control strategies in diesel engines, Renewable and Sustainable Energy Reviews 38 (2014) 732 – 746. doi:10.1016/j.rser.2014.07.019.

[15] J. H. Mack, D. Schuler, R. H. Butt, R. W. Dibble, Experimental investigation of butanol isomer combustion in Homogeneous Charge Compression Ignition (HCCI) engines, Applied Energy 165 (2016) 612 – 626. doi:10.1016/j.apenergy.2015.12.105.

[16] M. Shahbakhti, R. Lupul, C. R. Koch, Predicting HCCI Auto-Ignition Timing by Extending a Modified Knock-Integral Method, SAE Technical Paper 2007-01-0222. doi:10.4271/2007-01-0222.

[17] N. Morgan, A. Smallbone, A. Bhave, M. Kraft, R. Cracknell, G. Kalghatgi, Mapping surrogate gasoline compositions into RON/MON space, Combustion and Flame 157 (6) (2010) 1122 – 1131. doi:10.1016/j.combustflame.2010.02.003.

[18] Y. Han, S. Hu, M. Tan, Y. Xu, J. Tian, R. Li, J. Chai, J. Liu, X. Yu, Experimental study of the effect of gasoline components on fuel economy, combustion and emissions in gdi engine, Fuel 216 (2018) 371 – 380. doi:10.1016/j.fuel.2017.12.033.

[19] Z. Gong, L. Feng, Z. Wang, Experimental and numerical study of the effect of injection strategy and intake valve lift on superknock and engine performance in a boosted gdi engine, Fuel 249 (2019) 309 – 325. doi:10.1016/j.fuel.2019.03.005.

[20] T. Cerri, G. DErrico, A. Onorati, Experimental investigations on high octane number gasoline formulations for internal combustion engines, Fuel 111 (2013) 305 – 315. doi:10.1016/j.fuel.2013.03.065.

[21] J. Herzler, M. Fikri, K. Hitzbleck, R. Starke, C. Schulz, P. Roth, G. Kalghatgi, Shock-tube study of the autoignition of n-heptane/toluene/air mixtures at intermediate temperatures and high pressures, Combustion and Flame 149 (1) (2007) 25 – 31. doi:10.1016/j.combustflame.2006.12.015.

[22] S. K. Vallabhuni, A. D. Lele, V. Patel, A. Lucassen, K. Moshammer, M. AlAbbad, A. Farooq, R. X. Fernandes, Autoignition studies of Liquefied Natural Gas (LNG) in a shock tube and a rapid compression machine, Fuel 232 (2018) 423 – 430. doi:10.1016/j.fuel.2018.04.168.

[23] A. Lifshitz, K. Scheller, A. Burcat, G. B. Skinner, Shock-tube investigation of ignition in methane-oxygen-argon mixtures, Combustion and Flame 16 (1971) 311 – 321.

[24] S. S. Goldsborough, A chemical kinetically based ignition delay correlation for iso-octane covering a wide range of conditions including the NTC region, Combustion and Flame 156 (2009) 1248 – 1262. doi:10.1016/j.combustflame.2009.01.018.

[25] A. Douaud, P. Eyzat, Four-Octane-Number Method for Predicting the Anti-Knock Behavior of Fuels and Engines, SAE Transactions 87 (1978) 294–308.
URL https://www.jstor.org/stable/44734267

[26] A. D. B. Yates, C. L. Viljoen, An Improved Empirical Model for Describing Auto-ignition, SAE Technical Paper 2008-01-1629.

doi:10.4271/2008-01-1629.

[27] D. F. Davidson, S. C. Ranganath, K.-Y. Lam, M. Liaw, Z. Hong, R. K. H., Ignition Delay Time Measurements of Normal Alkanes and Simple Oxygenates, Journal of Propulsion and Power 26 (2) (2010) 280 – 287. doi:10.2514/1.44034.

[28] W. Burwell, D. Olson, The Spontaneous Ignition of Isooctane Air Mixtures under Steady Flow Conditions, SAE Technical Paper 650510. doi:10.4271/650510.

[29] D. R. Haylett, D. F. Davidson, R. K. Hanson, Ignition delay times of low-vapor-pressure fuels measured using an aerosol shock tube, Combustion and Flame 159 (2) (2012) 552 – 561. doi:10.1016/j.combustflame.2011.08.021.

[30] J. B. Heywood, Internal Combustion Engine Fundamentals, McGraw Hill, United States of America, 1988.

[31] I. Glassman, R. A. Yetter, N. G. Glumac, Combustion, Vol. Fifth edition, Academic Press, United States of America, 2014.

[32] V. Nayagam, D. L. Dietrich, M. C. Hicks, F. A. Williams, Coolflame extinction during n-alkane droplet combustion in microgravity, Combustion and Flame 162 (5) (2015) 2140 – 2147. doi:10.1016/j.combustflame.2015.01.012.

[33] A. Brassat, M. Thewes, M. Mther, S. Pischinger, C. Lee, R. X. Fernandes, H. Olivier, Y. Uygun, Analysis of the Effects of Certain Alcohol and Furan-Based Biofuels on Controlled Auto Ignition, SAE Technical Paper 2012-01-1135. doi:10.4271/2012-01-1135.

[34] C. Lee, A. Ahmed, E. F. Nasir, J. Badra, G. Kalghatgi, S. M. Sarathy, H. Curran, A. Farooq, Autoignition characteristics of oxygenated gasolines, Combustion and Flame 186 (2017) 114 – 128. doi:10.1016/j.combustflame.2017.07.034.

[35] L. R. Cancino, Development and application of detailed chemical kinetics mechanisms for ethanol and ethanol containing hydrocarbon fuels, Ph.D. thesis, Graduate Program in Mechanical Engineering, Federal University of Santa Catarina - POSMEC/UFSC (2009).
URL https://repositorio.ufsc.br/bitstream/handle/123456789/193034/Cancino%20L.R%202009%20-%20Ph.D%20Thesis.pdf?sequence=1&isAllowed=y

[36] M. Mehl, W. J. Pitz, C. K. Westbrook, H. J. Curran, Kinetic modeling of gasoline surrogate components and mixtures under engine conditions, Proceedings of the Combustion Institute 33 (1) (2011) 193 – 200. doi:10.1016/j.proci.2010.05.027.

[37] J. E. Dec, Y. Yang, J. Dernotte, C. Ji, Effects of gasoline reactivity and ethanol content on boosted, premixed and partially stratified low-temperature gasoline combustion (LTGC), SAE International Journal of Engines 8 (3) (2015) 935–955. doi:10.4271/2015-01-0813.

[38] K. Siokos, Z. He, R. Prucka, Assessment of model-based knock prediction methods for spark-ignition engines, SAE Technical Paper (2017-01-0791). doi:10.4271/2017-01-0791.

[39] B. Wang, M. Pamminger, T. Wallner, Optimizing thermal efficiency of a multi-cylinder heavy duty engine with E85 gasoline compression ignition, SAE Technical Paper (2019-01-0557). doi:10.4271/2019-01-0557.

[40] E. Agbro, A. S. Tomlin, M. Lawes, S. Park, S. M. Sarathy, The influence of n-butanol blending on the ignition delay times of gasoline and its surrogate at high pressures, Fuel 187 (2017) 211–219. doi:10.1016/j.fuel.2016.09.052.

[41] S. M. Sarathy, G. Kukkadapu, M. Mehl, T. Javed, A. Ahmed, N. Naser, A. Tekawade, G. Kosiba, M. AlAbbad, E. Singh, S. Park, M. A. Rashidi, S. H. Chung, W. L. Roberts, M. A. Oehlschlaeger, C.-J. Sung, A. Farooq, Compositional effects on the ignition of FACE gasolines, Combustion and Flame 169 (2016) 171–193. doi:10.1016/j.combustflame.2016.04.010.

[42] A. da Silva Jr., J. Hauber, L. Cancino, K. Huber, The research octane numbers of ethanol-containing gasoline surrogates, Fuel 243 (2019) 306 – 313. doi:10.1016/j.fuel.2019.01.068.

[43] W. J. Pitz, N. P. Cernansky, F. L. Dryer, F. N. Egolfopoulos, J. T. Farrell, D. G. Friend, H. Pitsch, Development of an Experimental Database and Chemical Kinetic Models for Surrogate Gasoline Fuels, SAE Technical Paper 2007-01-0175. doi:10.4271/2007-01-0175.

[44] W. K. Metcalfe, W. J. Pitz, H. J. Curran, J. M. Simmie, C. K. Westbrook, The development of a detailed chemical kinetic mechanism for diisobutylene and comparison to shock tube ignition times, Proceedings of the Combustion Institute 31 (1) (2007) 377 – 384. doi:10.1016/j.proci.2006.07.207.

[45] C. Pera, V. Knop, Methodology to define gasoline surrogates dedicated to auto-ignition in engines, Fuel 96 (2012) 59 – 69. doi:10.1016/j.fuel.2012.01.008.

[46] W. Adao, L. Cancino, Spray behavior on compression ignition internal combustion engines: a cfd analysis of cavitation in the fuel injector, in: Proceedings of the 25th International Congress of Mechanical Engineering, no. paper COB-2019-2161, Associação Brasileira de Engenharía e Ciências Mecânicas, ABCM, 2019.

[47] J. Henschel, L. Cancino, Numerical analysis of fuel spray angle on the operating parameters in a locomotive diesel engine, in: Proceedings of the 25th International Congress of Mechanical Engineering, no. paper COB-2019-1642, Associação Brasileira de Engenharía e Ciências Mecânicas, ABCM, 2019.

[48] M. Jia, M. Xie, A chemical kinetics model of iso-octane oxidation for hcci engines, Fuel 85 (17-18) (2006) 2593 – 2604. doi:10.1016/j.fuel.2006.02.018.

[49] L. Cancino, M. Fikri, A. Oliveira, C. Schulz, Ignition delay times of ethanol-containing multi-component gasoline surrogates: Shock-tube experiments and detailed modeling, Fuel 90 (3) (2011) 1238 – 1244. doi:10.1016/j.fuel.2010.11.003.

[50] S. M. Sarathy, A. Farooq, G. T. Kalghatgi, Recent progress in gasoline surrogate fuels, Progress in Energy and Combustion Science 65 (2018) 67 – 108. doi:10.1016/j.pecs.2017.09.004.

[51] D. B. Lenhert, D. L. .Miller, N. P. Cernansky, K. G. Owens, The oxidation of a gasoline surrogate in the negative temperature coefficient region, Combustion and Flame 156 (2009) 549 – 564. doi:10.1016/j.combustflame.2008.11.022.

[52] M. Fikri, J. Herzler, R. Starke, C. Schulz, P. Roth, G. T. Kalghatgi, Autoignition of gasoline surrogates mixtures at intermediate temperatures and high pressures, Combustion and Flame 152 (2008) 276 – 281. doi:10.1016/j.combustflame.2007.07.010.

[53] H. Li, Y. Qiu, Z. Wu, S. Wang, X. Lu, Z. Huang, Ignition delay of diisobutylene-containing multicomponent gasoline surrogates: Shock tube measurements and modeling study, Fuel 235 (2019) 1387 – 1399. doi:10.1016/j.fuel.2018.08.132.

[54] M. Su, C. P. Chen, Heating and evaporation of a new gasoline surrogate fuel: A discrete multicomponent modeling study, Fuel 161 (2015) 215 – 221. doi:10.1016/j.fuel.2015.08.048.

[55] M. Yahyaoui, N. Djebali-Chaumeix, P. Dagaut, C.-E.Paillard, S. Gail, Experimental and modelling study of gasoline surrogate mixtures oxidation in jet stirred reactor and shock tube, Proceedings of the Combustion Institute 31 (2007) 385 – 391. doi:10.1016/j.proci.2006.07.179.

[56] M. Feng, X. Z. Jiang, W. Zeng, K. H. Luo, P. Hellier, Ethanol oxidation with high water content: A reactive molecular dynamics simulation study, Fuel 235 (2019) 515 – 521. doi:10.1016/j.fuel.2018.08.040.

[57] M. Ko, Y. Sekmen, T. Topgl, H. S. Ycesu, The effects of ethanolunleaded gasoline blends on engine performance and exhaust emissions in a spark-ignition engine, Renewable Energy 34 (2009) 2101 – 2106. doi:10.1016/j.renene.2009.01.018.

[58] M. Aghsaee, D. Nativel, M. Bozkurt, M. Fikri, N. Chaumeix, C. Schulz, Experimental study of the kinetics of ethanol pyrolysis and oxidation behind reflected shock waves and in laminar flames, Proceedings of the Combustion Institute 35 (2015) 393 – 400. doi:10.1016/j.proci.2014.05.063.

[59] Y. Shen, E. King, U. Pfahl, Fuel Chemistry Impacts on Gasoline HCCI Combustion with Negative Valve Overlap and Direct Injection, SAE Technical Paper 2007-01-4105. doi:10.4271/2007-01-4105.

[60] A. M. Hochhauser, Review of Prior Studies of Fuel Effects on Vehicle Emissions, SAE Int. J. Fuels Lubr. 2 (2009) 541 – 567.
URL www.jstor.org/stable/26273409

[61] R. Perry, I. L.Gee, Vehicle emissions in relation to fuel compo-

sition, Science of The Total Environment 169 (1995) 149 – 156. doi:10.1016/0048-9697(95)04643-F.

[62] J. G. Speight, The Chemistry and Technology of Petroleum, Vol. Fifth edition, CRC Press, 2014.

[63] R. Sadeghbeigi, Fluid Catalytic Cracking Handbook, Vol. Third edition, Butterworth Heinemann, 2012.

[64] L. Cancino, M. Fikri, A. Oliveira, C. Schulz, Autoignition of gasoline surrogate mixtures at intermediate temperatures and high pressures: Experimental and numerical approaches, Proceedings of the Combustion Institute 32 (1) (2009) 501 – 508. doi:10.1016/j.proci.2008.06.180.

[65] L. Cancino, M. Fikri, A. Oliveira, C. Schulz, Computational fluid dynamic simulation of a non-reactive propagating shock wave in a shock tube, in: Proceedings of the 27th International Symposium on Shock Waves - ISSW27, The Ioffe Institute of Russian Academy of Sciences, IOFFE, 2009.
URL https://repositorio.ufsc.br/bitstream/handle/123456789/193042/ISSW27_CFD_shock_wave_Leonel.pdf?sequence=1&isAllowed=y

[66] L. Cancino, M. Fikri, A. Oliveira, C. Schulz, Autoignition of binary mixtures of gasoline surrogates,ethanol iso-octane blends in air: Numerical and experimental study in a high-pressure shock tube, in: Proceedings of the 20th International Congress of Mechanical Engineering, Associação Brasileira de Engenharía e Ciências Mecânicas, ABCM, 2009.
URL https://repositorio.ufsc.br/bitstream/handle/123456789/193044/COB09-0355%20-%20COBEM2009%20-%20Leonel.pdf?sequence=1&isAllowed=y

[67] A. De Toni, M. Werler, R. Hartmann, L. Cancino, R. Schiessl, M. Fikri, C. Schulz, A. Oliveira, E. Oliveira, M. Rocha, Ignition delay times of Jet A-1 fuel: Measurements in a high-pressure shock tube and a rapid compression machine, Proceedings of the Combustion Institute 36 (3) (2017) 3695 – 3703. doi:10.1016/j.proci.2016.07.024.

[68] H. Nakamura, D. Darcy, M. Mehl, C. J. Tobin, W. K. Metcalfe, W. J. Pitz, C. K. Westbrook, H. J. Curran, An experimental and modeling study of shock tube and rapid compression machine ignition of n-butylbenzene/air mixtures, Combustion and Flame 161 (1) (2014) 49 – 64. doi:10.1016/j.combustflame.2013.08.002.

[69] D. Darcy, M. Mehl, J. Simmie, J. Wrmel, W. Metcalfe, C. Westbrook, W. Pitz, H. Curran, An experimental and modeling study of the shock tube ignition of a mixture of n-heptane and n-propylbenzene as a surrogate for a large alkyl benzene, Proceedings of the Combustion Institute 34 (1) (2013) 411 – 418. doi:10.1016/j.proci.2012.06.131.

[70] K. Zhang, C. Banyon, C. Togb, P. Dagaut, J. Bugler, H. J. Curran, An experimental and kinetic modeling study of n-hexane oxidation, Combustion and Flame 162 (11) (2015) 4194 – 4207. doi:10.1016/j.combustflame.2015.08.001.

[71] M. F. Campbell, T. Parise, A. M. Tulgestke, R. M. Spearrin, D. F. Davidson, R. K. Hanson, Strategies for obtaining long constant-pressure test times in shock tubes, Shock Waves 25 (6) (2015) 651–665. doi:10.1007/s00193-015-0596-x.

[72] R. Kee, F. Rupley, J. Miller, Chemkin-II: A Fortran Chemical Kinetics Package for the Analysis of Gas-Phase Chemical Kinetics, Technical Report SAND89-8009.UC-401, SANDIA (September 1989).

[73] D. Davidson, M. Oehlschlaeger, J. Herbon, R. Hanson, Shock tube measurements of iso-octane ignition times and oh concentration time histories, Proceedings of the Combustion Institute 29 (1) (2002) 1295 – 1301. doi:10.1016/S1540-7489(02)80159-6.

[74] V. Vasudevan, D. Davidson, R. Hanson, Shock tube measurements of toluene ignition times and oh concentration time histories, Proceedings of the Combustion Institute 30 (1) (2005) 1155 – 1163. doi:10.1016/j.proci.2004.07.039.

[75] H. Mirels, Test time in low-pressure shock tubes, The Physics of Fluids 6 (9) (1963) 1201–1214. doi:10.1063/1.1706887.

[76] E. Petersen, R. Hanson, Nonideal effects behind reflected shock waves in a high-pressure shock tube, Shock Waves 10 (6) (2001) 405–420. doi:10.1007/PL00004051.

[77] D. G. Goodwin, R. L. Speth, H. K. Moffat, B. W. Weber, Cantera: An object-oriented software toolkit for chemical kinetics, thermodynamics, and transport processes, https://www.cantera.org, version 2.4.0 (2018). doi:10.5281/zenodo.1174508.

[78] L. R. Cancino, M. Fikri, A. A. M. Oliveira, C. Schulz, Measurement and chemical kinetics modeling of shock-induced ignition of ethanol-air mixtures, Energy & Fuels 24 (5) (2010) 2830–2840. doi:10.1021/ef100076w.

[79] E. Ranzi, A. Frassoldati, R. Grana, A. Cuoci, T. Faravelli, A. Kelley, C. Law, Hierarchical and comparative kinetic modeling of laminar flame speeds of hydrocarbon and oxygenated fuels, Progress in Energy and Combustion Science 38 (4) (2012) 468 – 501. doi:10.1016/j.pecs.2012.03.004.

[80] A. Frassoldati, A. Cuoci, T. Faravelli, U. Niemann, E. Ranzi, R. Seiser, K. Seshadri, An experimental and kinetic modeling study of n-propanol and iso-propanol combustion, Combustion and Flame 157 (1) (2010) 2 – 16. doi:10.1016/j.combustflame.2009.09.002.

[81] E. Ranzi, A wide-range kinetic modeling study of oxidation and combustion of transportation fuels and surrogate mixtures, Energy & Fuels 20 (3) (2006) 1024–1032. doi:10.1021/ef060028h.

[82] M. Fikri, J. Herzler, R. Starke, C. Schulz, P. Roth, G. Kalghatgi, Autoignition of gasoline surrogates mixtures at intermediate temperatures and high pressures, Combustion and Flame 152 (1) (2008) 276 – 281. doi:10.1016/j.combustflame.2007.07.010.

[83] E. Petersen, D. Davidson, R. Hanson, Kinetics modeling of shock-induced ignition in low-dilution ch4/o2 mixtures at high pressures and intermediate temperatures, Combustion and Flame 117 (1) (1999) 272 – 290. doi:10.1016/S0010-2180(98)00111-4.

[84] M. Yahyaoui, N. Djebaili-Chaumeix, C.-E. Paillard, S. Touchard, R. Fournet, P. Glaude, F. Battin-Leclerc, Experimental and modeling study of 1-hexene oxidation behind reflected shock waves, Proceedings of the Combustion Institute 30 (1) (2005) 1137 – 1145. doi:10.1016/j.proci.2004.08.070.

[85] D. Davidson, J. Shao, R. Choudhary, M. Mehl, N. Obrecht, R. Hanson, Ignition delay time measurements and modeling for gasoline at very high pressures, Proceedings of the Combustion Institute 37 (4) (2019) 4885 – 4892. doi:https://doi.org/10.1016/j.proci.2018.08.032.

[86] S. M. Sarathy, G. Kukkadapu, M. Mehl, W. Wang, T. Javed, S. Park, M. A. Oehlschlaeger, A. Farooq, W. J. Pitz, C.-J. Sung, Ignition of alkane-rich face gasoline fuels and their surrogate mixtures, Proceedings of the Combustion Institute 35 (1) (2015) 249 – 257. doi:https://doi.org/10.1016/j.proci.2014.05.122.